J. Physiol. (1960), **151**, *pp.* 491–501
With 5 text-figures
Printed in Great Britain

QUANTITATIVE DESCRIPTION OF SODIUM CURRENTS IN MYELINATED NERVE FIBRES OF *XENOPUS LAEVIS*

BY B. FRANKENHAEUSER

From the Nobel Institute for Neurophysiology, Karolinska Institutet, Stockholm 60, Sweden

(*Received* 14 *December* 1959)

Earlier experiments (Dodge & Frankenhaeuser, 1959) on the myelinated nerve fibre demonstrated that the initial ionic current is caused by sodium ions moving passively down their electro-chemical gradient. These studies, carried out by using the voltage clamp technique, also showed that (1) the sodium-carrying mechanism can be described in terms of the sodium permeability (P_{Na}) of the membrane, when the permeability is calculated from the constant-field equation for a simple membrane, (2) the sodium permeability depends on the membrane potential and (3) the permeability changes with finite speed in response to a change in membrane potential. Further studies were concerned with the effect of conditioning polarization on the available sodium permeability (Frankenhaeuser, 1959).

The present investigation is concerned with the time course of the change in sodium permeability. The recorded current consists of a capacitive current, an unspecific leak current, a sodium current and a delayed ionic current. Before further analysis can be carried out, sodium current has to be separated out from the other currents. The capacitive current and the leak current can be estimated from records taken with anodal pulses and subtracted from the recorded total currents. At times later than the peak of the initial current the delayed ionic current begins. In order to separate the sodium current from the delayed ionic current it is necessary either that the delayed current should be determined independently, as can be done in low external sodium concentrations (Hodgkin & Huxley, 1952*a*; Dodge & Frankenhaeuser, 1959), or that the time course of the sodium permeability change should be determined from the instantaneous current–voltage relations by means of records taken at sudden repolarizations to a value of membrane potential that is near the equilibrium potential for the delayed current (Hodgkin & Huxley, 1952*b*; Dodge & Frankenhaeuser, 1958). The latter method, although more elaborate, was preferred in the present investigation, since experiments with choline solutions showed some diminution of the delayed ionic current that would have given an apparent reversal of sodium current at later times for large cathodal

pulses. This effect suggests that choline chloride is a not altogether inert replacement for sodium. The time course of the change of P_{Na} was hence determined at various times during a number of different polarizations and the rate constants α_m, β_m, α_h and β_h which determined P_{Na} were calculated. The formal assumptions made for this calculation are very closely related to those made for the squid fibre voltage-clamp data (Hodgkin & Huxley, 1952*d*). Empirical equations were then fitted to the experimental data. This set of equations ought to describe the sodium currents for any time course of potential change within the potential range investigated. The total ionic currents cannot, however, be described before the delayed currents have been treated quantitatively. The delayed currents will be analysed in a subsequent paper.

METHODS

The membrane potential of a node in a large myelinated nerve fibre from the sciatic nerve of *Xenopus laevis* was changed in rectangular steps. The membrane potential was controlled by a feed-back amplifier system (Dodge & Frankenhaeuser, 1958, 1959) and the current calibration was made as previously described (Dodge & Frankenhaeuser, 1959).

The Ringer's solution had the following composition (mM): NaCl 112·0, KCl 2·5, $CaCl_2$ 2·0, $NaHCO_3$ 2·5.

Procedure. Several clamp runs were taken in each experiment. (*a*) The pulse amplitude was varied (e.g. Dodge & Frankenhaeuser, 1959, Fig. 1). The sodium equilibrium potential (V_{Na}), the curve relating peak sodium current to membrane potential (I_{Na}–V_m curve), and the curve relating peak sodium permeability to membrane potential (P_{Na}–V_m curve) were obtained from these records (e.g. Dodge & Frankenhaeuser, 1959, Figs. 2 and 3). (*b*) The membrane potential was changed in two steps. The first, conditioning, step polarized the membrane to various values, while the second, test, step took V to a value close to that potential at which sodium current was at its maximum (as a rule to $V = +57$ mV). The curve for steady state inactivation against membrane potential (h_∞–V_m curve) was obtained from these records (e.g. Hodgkin & Huxley, 1952*c*, Fig. 5; Frankenhaeuser, 1959, Fig. 3). (*c*) Double pulses were applied, by means of which conditioning polarizations of various amplitudes and various durations preceded a test step, making $V = +57$ mV (at which potential the initial inward current is maximal). The time course of inactivation at various membrane potentials was determined from this run (e.g. Hodgkin & Huxley, 1952*c*, Fig. 3; Dodge & Frankenhaeuser, 1958, Fig. 8). (*d*) Pulses of various amplitudes were applied and interrupted at various times after the onset. The repolarization gave a tail of sodium current (e.g. Hodgkin & Huxley, 1952*b*, Fig. 10; Dodge & Frankenhaeuser, 1958, Fig. 9) from which the time course of the P_{Na} change was determined. (*e*) Anodal pulses were applied. Capacitive currents and leak currents were estimated from these records. (*f*) A number of runs were taken for an analysis of the delayed currents. These will be treated in a subsequent paper.

The order in which runs were taken was varied from experiment to experiment. All the runs were not taken in each individual experiment. Systematic runs were taken on about 40 axons. As a rule interest was concentrated in order to establish single details rather than to give a complete quantitative analysis, and quite a number of experiments were made at temperatures other than room temperature. Towards the end of the experimental series a few experiments were made so as to give a relatively complete over-all picture at room temperature (20° C). These experiments were by no means the most stable ones, and scatter

between measured points was less in many other experiments. However, it was decided to concentrate for the quantitative description in the present paper on the data obtained from these four axons.

Axons were numbered in order to allow comparison of data between figures and tables in the two preceding papers and in this one. The numbers were not in chronological order of experiments.

Nomenclature. Potentials are given as inside potential minus outside potential, and outward current as positive. E is used for absolute values of potentials. V is used for potentials relative to the resting potential, thus $V = E - E_r$.

FORMAL TREATMENT AND ASSUMPTIONS

A number of formal assumptions were made in order to make it possible to derive the empirical equations that describe the sodium currents in the myelinated nerve. These assumptions were intended to be as closely related as possible to those made by Hodgkin & Huxley (1952*d*) for the squid fibre voltage-clamp data.

In a previous paper (Dodge & Frankenhaeuser, 1959) it was shown that the sodium-carrying properties of the membrane at the time of the peak of the initial ionic current could be satisfactorily described by the sodium permeability (P_{Na}) of the membrane with the constant-field equation. The assumptions required for this conclusion are those required for the derivation of the constant-field equation, and the assumption that P_{Na} of the membrane changes with finite speed. A further step is to assume that Na concentration changes rapidly within the membrane, and reaches a steady state so quickly that the transients can be neglected. Considering the dimensions of the membrane this is a plausible approximation, and the observations have been consistent with the idea; but it must be emphasized that the resolution of the technique is severely limited at very short times ($< 0{\cdot}02$ msec) after the voltage step is applied. The sodium current (I_{Na}) would thus at any instant and at any membrane potential be determined by the P_{Na} of the membrane according to the constant-field equation. Thus

$$I_{Na} = P_{Na} \frac{F^2 E}{RT} [Na]_0 \frac{\exp\{(E - E_{Na}) F/RT\} - 1}{\exp\{EF/RT\} - 1}. \qquad (1)$$

Sodium current is thus linearly related to P_{Na} at any one voltage-clamp step (since E is held constant during step). Changes in P_{Na} with time can thus be determined from measurements of I_{Na}, and it is clear from the earlier measurements that P_{Na} changes continuously with time and with membrane potential.

For cathodal steps, sodium current rises with an S-shaped time course and is transient, whereas for a repolarization sodium current decays with an exponential time course. In order to obtain a formal equation which accounts for this, it was assumed by analogy with the treatment of the

squid fibre data (Hodgkin & Huxley, 1952*d*) that P_{Na} is a power function of a first-order equation. The time course of the sodium current was compared with a family of curves with the form

$$(1-\exp\{-t/\tau_1\})^a \times \exp\{-t/\tau_2\}.$$

This revealed that $a = 2$ gave a somewhat better fit with the experimental points than $a = 3$, which was used for the squid fibre data. The delay in rise of the sodium current in the *Xenopus* fibre was thus found to be somewhat smaller than in the squid fibre.

Thus

$$P_{Na} = \bar{P}_{Na}\, m^2 h, \tag{2}$$

$$\frac{dm}{dt} = \alpha_m (1-m) - \beta_m m, \tag{3}$$

$$\frac{dh}{dt} = \alpha_h (1-h) - \beta_h h; \tag{4}$$

where $\bar{P}_{Na}$ is a constant with dimensions of permeability and has the numerical value that P_{Na} would take if $m = 1$ and $h = 1$; m and h are dimensionless variables which can vary between 0 and 1; α_m and β_m, and α_h and β_h, are rate constants which vary with membrane potential but not with time, and have dimensions of (time)$^{-1}$.

During a voltage-clamp step, V changes suddenly and then remains constant. α_m, β_m, α_h and β_h then change instantly to a new value that is appropriate to the new value of the membrane potential. The solutions for equations (3) and (4), when $m = m_0$ and $h = h_0$ at $t = 0$, are then

$$m = m_\infty - (m_\infty - m_0) \exp(-t/\tau_m), \tag{5}$$

$$h = h_\infty - (h_\infty - h_0) \exp(-t/\tau_h), \tag{6}$$

where

$$m_\infty = \alpha_m/(\alpha_m+\beta_m), \tag{7}$$

$$\tau_m = 1/(\alpha_m+\beta_m), \tag{8}$$

$$h_\infty = \alpha_h/(\alpha_h+\beta_h), \tag{9}$$

and

$$\tau_h = 1/(\alpha_h+\beta_h). \tag{10}$$

Combining equations (7) and (8),

$$\alpha_m = \frac{m_\infty}{\tau_m} \quad \text{and} \quad \beta_m = (1-m_\infty)/\tau_m. \tag{11), (12}$$

Combining equations (9) and (10),

$$\alpha_h = \frac{h_\infty}{\tau_h} \quad \text{and} \quad \beta_h = (1-h_\infty)/\tau_h. \tag{13), (14}$$

As a rule the membrane potential was at its resting value before the pulse was applied, and at this potential m was negligibly small compared

with its maximal value during the pulse. m_0 could therefore be neglected when the pulse was larger than about $+30$ mV, and h_∞ was nearly zero for such pulses. In this case the solution of equation (2) is:

$$P_{Na} = P'_{Na}\{1-\exp(-t/\tau_m)\}^2 \{\exp(-t/\tau_h)\}, \quad (15)$$

where $P'_{Na} = \bar{P}_{Na} m_\infty^2 h_0$, that is to say P'_{Na} has the value which the P_{Na} would attain if inactivation were to remain at its resting value.

METHOD OF ANALYSIS

Voltage-clamp runs (*a–f*) were taken as described on p. 492, and the following data were extracted from the records and tabulated: *A*. The peak $I_{Na}-V$ relation was measured from runs (*a*) and (*e*). *B*. The sodium equilibrium potential V_{Na} or E_{Na} was determined from (*a*) and (*e*). *C*. The peak $P_{Na}-V$ relation was calculated from equation (1) by using the data in *A* and *B*. *D*. The steady state $h_\infty-V$ relation was measured from runs (*b*) and (*e*). *E*. The time constant for the change of h, τ_h, at various values of V between about -50 and $+40$ mV, was measured from runs (*c*) and (*e*). *F*. The time course of the change of P_{Na} at various potentials was determined from runs (*d*) and (*e*). *G*. The data obtained in *F* were plotted on double-log. paper and compared with a plot of a family of solutions of equation (15) with various values of τ_m/τ_h. *H*. P'_{Na} was obtained from *C* and *G*. *I*. $\bar{P}_{Na}$ was obtained from *C*, *D* and *G*. *K*. The $m_\infty-V$ relation was obtained from *H*, m_∞ being the square root of the ratio of P'_{Na} to the asymptote value of P'_{Na} at large cathodal pulses. *L*. τ_m and τ_h were obtained from *G*. *M*. The values of α_m, β_m, α_h and β_h were then calculated from equations (11), (12), (13) and (14).

RESULTS

The experimental values for the four rate constants are plotted against V in Figs. 1–4, m_∞ is plotted against V in Fig. 5, and the values of P_{Na} and V_{Na} are given in Table 1. The asymptote value of P'_{Na} at large pulses was determined by drawing a smooth line through a number of single determinations of P'_{Na} at large cathodal pulses, and the value of maximally available I_{Na} was determined from a smooth line drawn through the peak currents with a number of large anodal conditioning polarizations. Otherwise the calculation of the individual values in Fig. 1–5 was based on 'single point observations'.

The next step was to fit empirical equations to the experimental values of the rate constants. It seemed clear that α_m, β_m and β_h could reasonably well be fitted with a common curve for all the individual fibres, while the values for α_h fell on separate curves for the individual fibres.

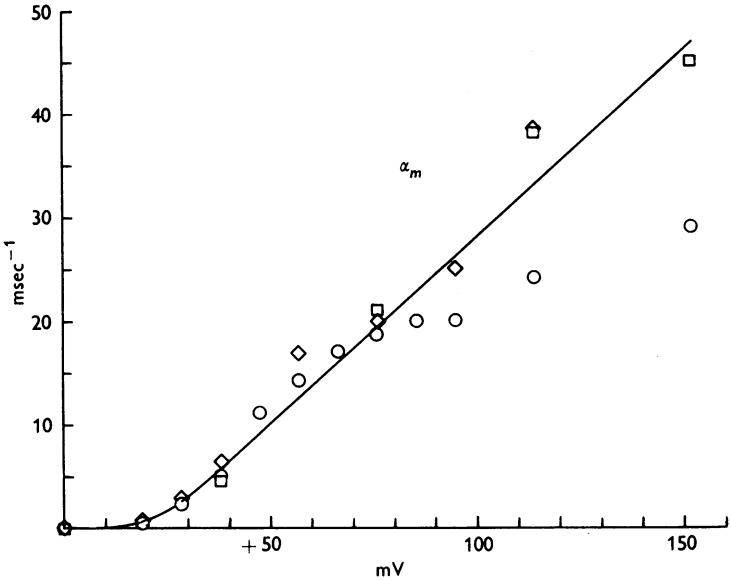

Fig. 1. Rate constant α_m of sodium permeability plotted against V. Continuous line is the solution of equation (16). 20° C. Axon 10 ◇, 11 □, 12 ○.

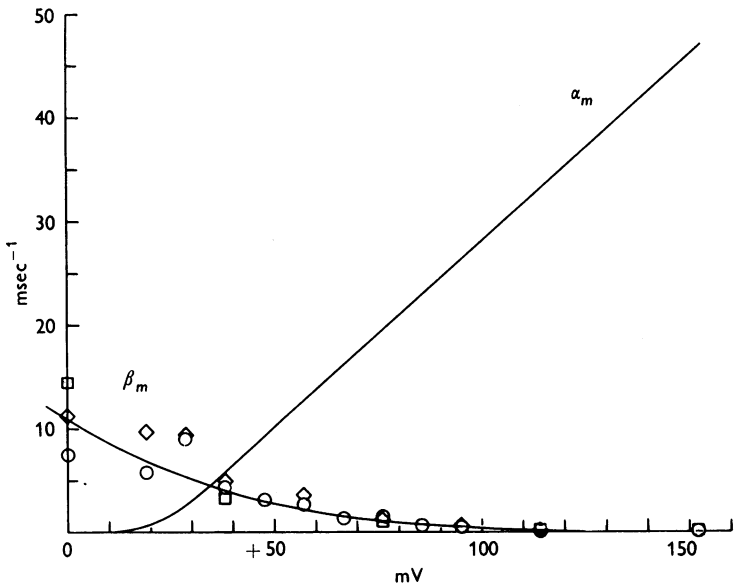

Fig. 2. Rate constant β_m of sodium permeability plotted against V. The continuous line for β_m drawn as solution of equation (17). The curve for α_m drawn in for comparison. 20° C. Axon 10 ◇, 11 □, 12 ○.

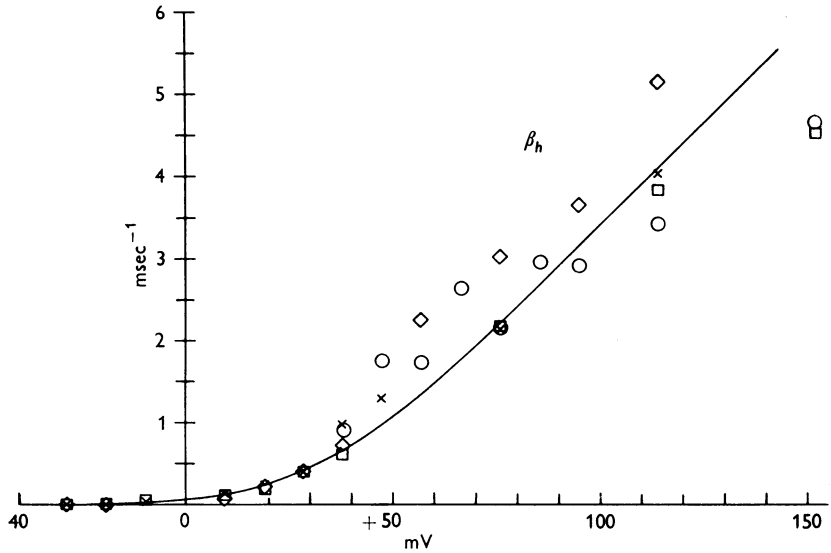

Fig. 3. Rate constant β_h of inactivation plotted against V. The continuous line for β_h drawn as solution of equation (19). 20° C. Axon 9 ×, 10 ◇, 11 □, 12 ○.

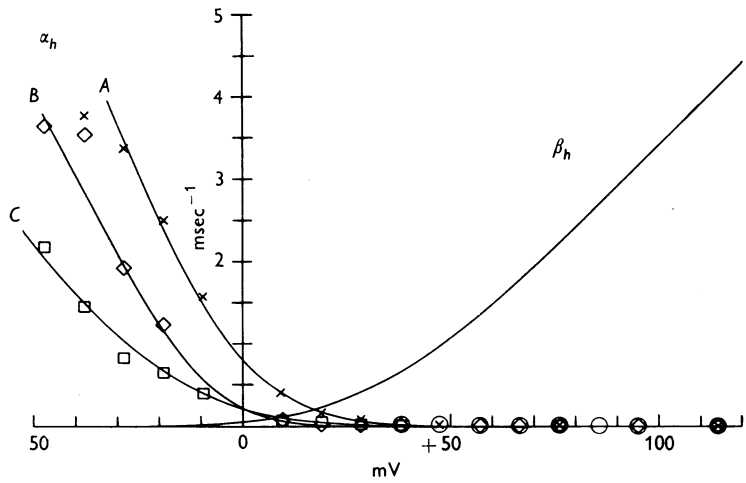

Fig. 4. Rate constant α_h of inactivation plotted against V. Continuous lines for α_h drawn as solutions of equation (18). The curve for β_h drawn in for comparison. 20° C. Axon 9 ×, 10 ◇, 11 □, 12 ○.

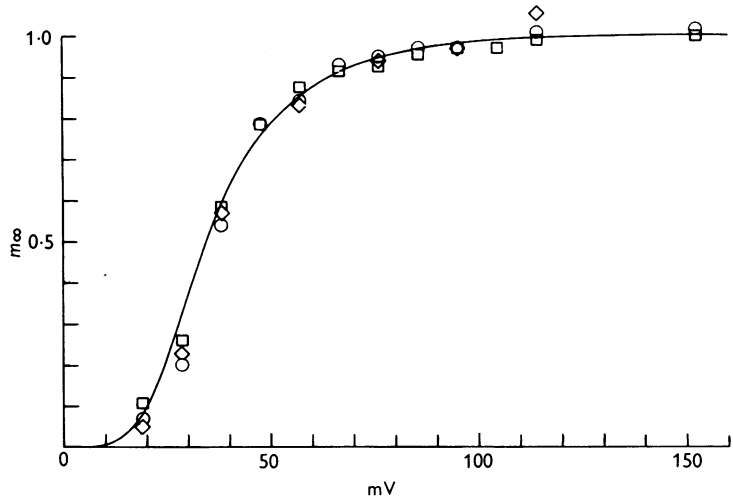

Fig. 5. m_∞ plotted against V. Continuous line drawn as solution of equation (7). 20° C. Axon 10 ◇, 11 □, 12 ○.

TABLE 1

Axon	P_{Na} (cm/sec; $\times 10^{-3}$)	P'_{Na} (cm/sec; $\times 10^{-3}$)	$\bar{P}_{Na}$ (cm/sec; $\times 10^{-3}$)	V_{Na} (mV)	E_{Na} (mV)	$g_L = \frac{I_L}{E-E_R}$ (m-mho/cm²)
9	4·0	6·0	6·7	+126·2	+56·2	25·4
10	2·9	5·1	6·6	+120·0	+50·0	26·5
11	2·5	3·6	6·1	+125·0	+55·0	28·2
12	4·6	8·2	12·4	+120·2	+50·2	41·0
Mean	3·5	5·7	8·0	+122·9	+52·9	30·3

E_R is taken as −70 mV. Some of the values deviate from values given for corresponding axons in Table 1 of Frankenhaeuser (1959). Measurements were made on different runs, and no corrections have been made for deterioration of the fibres during the experiment.

The continuous lines in Figs. 1–5 are drawn according to the equations:

$$\alpha_m = 0{\cdot}36\,(V-22)\Big/\left\{1-\exp\left(\frac{22-V}{3}\right)\right\}, \tag{16}$$

$$\beta_m = 0{\cdot}4\,(13-V)\Big/\left\{1-\exp\left(\frac{V-13}{20}\right)\right\}, \tag{17}$$

$$\alpha_h = a(b-V)\Big/\left\{1-\exp\left(\frac{V-b}{c}\right)\right\}, \tag{18}$$

where the values of a, b and c were

Axon	Curve	a	b (mV)	c (mV)
9	A	0·14	− 5	+ 8
10	B	0·10	−10	+ 6
11	C	0·07	−20	+10

$$\beta_h = 0{\cdot}05\,(V-32)\Big/\left\{1-\exp\left(\frac{32-V}{10}\right)\right\} \tag{19}$$

and

$$m_\infty = \alpha_m/(\alpha_m+\beta_m), \tag{7}$$

where α_m and β_m have the values given by equations (16) and (17) in msec^{-1} at 20° C.

The equation (1) in the preceding paper (Frankenhaeuser, 1959) for the $h_\infty - V$ relation is an approximation for

$$h_\infty = \alpha_h/(\alpha_h+\beta_h), \tag{9}$$

where α_h and β_h have the values given by equations (17) and (18).

The general form of equation which was chosen for all the rate constants is the same as that used by Hodgkin & Huxley (1952*d*) for α_m (note the difference in nomenclature). β_h did not, as in the squid fibre data, reach a limiting value at high values of V. This was tested on other fibres to +180 mV. The membrane breaks down at slightly higher potentials, so it was impossible to check it at still higher values. α_h and β_m could not be fitted with simple exponential curves. This was especially the case when β_m was measured at −57 mV. (These experiments were made at other temperatures and are therefore not included in the figures of this paper.)

DISCUSSION

The rate constants that govern the sodium-carrying mechanism in the myelinated nerve are described by equations (16)–(19) as graded smooth functions of the membrane potential. There was a fair amount of scatter between the points in Figs. 1–4. This scatter was certainly due to small errors in the measurements and not due to a step-wise turn on (or off) of the permeability of certain regions of the membrane in an all-or-none manner, since the membrane currents were smoothly graded with time and also with membrane potential at very small (2 mV) changes in potential steps. The following question then arises: do these equations describe the sodium permeability changes in the single 'sodium channel' or do they describe the average behaviour of a great number of single channels? The possibilities of observing the behaviour of a single channel seems more favourable with isolated nodes than with squid fibres, since the surface area of the node is very small compared to the area on which measurements are made on the squid fibre. So far it can be said that the resolution of the technique was such that quantal responses of a size of 1% of the maximal inward currents could have been detected, but were not in fact seen. Therefore, the only conclusion that can be drawn is: *either* there are very many sites (> 100) that turn on their sodium permeability either in a graded or in a quantal fashion, *or* the number of sites is

small, but in this case each single site must show a graded change in permeability. The 'all-or-none responses' reported by Tasaki & Bak (1958) are of quite a different order of size and can hardly be caused by the response of single sites.

In the present treatment, P_{Na} was described as being proportional to m^2 (equation 2) because this gave a better fit with the experimental data than m^3. The sodium currents were slightly more delayed if the fibre was polarized anodally before applying the test pulse. The third power could conceivably be correct if some permeability were already turned on at the resting potential. The experiments did not give any indications in this direction. Therefore m^2 was used, and not m^3 as for the squid fibre data (Hodgkin & Huxley, 1952*d*).

It was shown that m_∞, α_m, β_m and β_h were nearly the same in all the fibres, while h_∞ and α_h varied from fibre to fibre. The threshold (i.e. the membrane potential at which a regenerative action potential develops) of the fibres did not vary much between individual fibres. Threshold potential mainly depends on α_m and β_m, if $\bar{P}_{Na}$ and non-specific permeability are the same for all the fibres. The response to linearly rising currents and the accommodation are again known to vary largely. This variation seems at present to be accounted for by the variation in α_h. (These conclusions are drawn with some reservation because a complete quantitative treatment cannot be made until the delayed currents have been analysed quantitatively.) Accommodation is commonly held to be closely associated with calcium, and the external calcium concentration is known to change the accommodation. Calcium, however, changes all the rate constants in squid axons (Frankenhaeuser & Hodgkin, 1957), while only α_h was found to vary from fibre to fibre. It seems therefore likely either that calcium has very little to do with the variation in accommodation in normal ionic environments, or that, if calcium plays an important part, then something else must compensate for the effect of calcium on α_m, β_m and β_h.

The empirical equations describing the relation of sodium permeability to membrane potential and to time are consistent with the idea that charged particles moving in an electric field govern the permeability changes. Further, the sodium permeability of the membrane appears to be independent of sodium concentration and independent of membrane current, and the permeability changes are smoothly graded with potential and with time. Thus these observations indicate that while there are some differences between the sodium permeability changes of the squid giant fibre and the frog myelinated nerve fibre nevertheless the similarities are very striking.

SUMMARY

1. The sodium currents (I_{Na}) were analysed in voltage-clamp experiments on the myelinated nerve fibre of *Xenopus laevis*. The analysis was made in terms of the sodium permeability (P_{Na}) of the membrane, and equations were fitted to the experimental data.

2. These empirical equations (2) to (19), describe how P_{Na} depended on membrane potential and on time.

3. The analysis indicates striking similarities in the sodium transport system in the frog fibre and in the squid fibre, although a number of differences were noted.

This investigation was supported by the Rockefeller Foundation and by Stiftelsen Therese och Johan Anderssons Minne.

REFERENCES

DODGE, F. A. & FRANKENHAEUSER, B. (1958). Membrane currents in isolated frog nerve fibre under voltage clamp conditions. *J. Physiol.* **143**, 76–90.

DODGE, F. A. & FRANKENHAEUSER, B. (1959). Sodium currents in the myelinated nerve fibre of *Xenopus laevis* investigated with the voltage clamp technique. *J. Physiol.* **148**, 188–200.

FRANKENHAEUSER, B. (1959). Steady state inactivation of sodium permeability in myelinated nerve fibres of *Xenopus laevis*. *J. Physiol.* **148**, 671–676.

FRANKENHAEUSER, B. & HODGKIN, A. L. (1957). The action of calcium on the electrical properties of squid axons. *J. Physiol.* **137**, 218–244.

HODGKIN, A. L. & HUXLEY, A. F. (1952*a*). Currents carried by sodium and potassium ions through the membrane of the giant axon of *Loligo*. *J. Physiol.* **116**, 449–472.

HODGKIN, A. L. & HUXLEY, A. F. (1952*b*). The components of membrane conductance in the giant axon of *Loligo*. *J. Physiol.* **116**, 473–496.

HODGKIN, A. L. & HUXLEY, A. F. (1952*c*). The dual effect of membrane potential on sodium conductance in the giant axon of *Loligo*. *J. Physiol.* **116**, 497–506.

HODGKIN, A. L. & HUXLEY, A. F. (1952*d*). A quantitative description of membrane current and its application to conduction and excitation in nerve. *J. Physiol.* **117**, 500–544.

TASAKI, I. & BAK, A. F. (1958). Current–voltage relations of single nodes of Ranvier as examined by voltage-clamp technique. *J. Neurophysiol.* **21**, 124–137.